Forestry An International Journal of Forest Research

Institute of Chartered Foresters

Forestry 2015; **88**, 180–189, doi:10.1093/forestry/cpu042
Advance Access publication 13 November 2014

The dynamics of structure across scale in a primaeval European beech stand

Eric K. Zenner[1]*, JeriLynn E. Peck[1], Martina L. Hobi[2] and Brigitte Commarmot[2]

[1]*Department of Ecosystem Science and Management, The Pennsylvania State University, University Park, PA 16802, USA*
[2]*Swiss Federal Institute of Forest, Snow, and Landscape Research WSL, 8903 Birmensdorf, Switzerland*

*Corresponding author. Tel: +41 18148654574; Fax: +41 18148653725; E-mail: Eric.Zenner@psu.edu

Received 1 May 2014

We explored the spatial dynamics of structural complexity in the living tree stratum in a 10-ha stem-mapped portion of an unmanaged nearly monospecific primaeval European beech (*Fagus sylvatica* L.) stand in Western Ukraine. Development dynamics were assessed through patterns of change in association across scales (from 156.25 m^2 to 1 ha) among stand basal area (BA), tree density, average and standard deviation (STD) of tree diameters, Gini coefficient (GC), the index of spatial aggregation (R), diameter differentiation index (T) and structural complexity index (SCI). At the smallest scales, STD, GC and *T* contrasted patches of differing structure (i.e. large between-patch structural differences). As subplot area increased and incorporated more heterogeneity, structural differences between subplots became more subtle and measures of tree-to-tree size variation (STD, T) lost sensitivity whereas it was gained for measures of overall within-patch heterogeneity (GC). At small scales, differences in STD largely explained variation in the SCI (between-plot variability); at intermediate scales, size differences among neighbours (*T*) explained most of the variability; and at large scales, plot-level differences in BA and its allocation to trees of different sizes (GC; within-plot variability) overrode size differences among nearest neighbours. The characterization of a fine-scale shifting mosaic of patches in different development stages appears to hold for primaeval beech forests in this spatially contiguous area of relatively large extent. The coalescence of small-scale processes into neighbourhoods, and then into patches at larger scales, may be best captured by the change in associations among structural measures across scales because the structural imprint of gap dynamics extends considerably beyond the scale of individual gaps.

Introduction

A proper understanding of the structural diversity of primaeval forests requires a multiscale ecological and spatial perspective (Spies, 2004) that can encompass the cumulative structural imprint of historic disturbances. Because disturbances and other processes of stand development operate at different spatial scales (Keane *et al*., 2009; Mori, 2011), coarse-scale studies are required to capture the signature of large-scale disturbances such as extensive wildfire or windthrow (Turner, 1989; Bengtsson *et al*., 2000), whereas smaller-scale studies are needed to focus attention on small-scale processes, such as gap partitioning dynamics, which may otherwise become smoothed out and overlooked at greater spatial extents (Busing and White, 1997). Primaeval forests are an ideal laboratory for explorations of temporal and spatial variability due to their long history and, often, high levels of diversity in structural condition (Spies, 2004; Zenner, 2005; Commarmot *et al*., 2013; Nagel *et al*., 2013). Natural European beech (*Fagus sylvatica* L.) forests have the additional appeal of simplifying the equation to a single, self-perpetuating shade tolerant species. European beech is also shade tolerant (Peters, 1997), withstanding multiple periods of suppression and release (Nagel *et al*., 2006; Wagner *et al*., 2010), including suppressed periods for upwards of 150 years (Trotsiuk *et al*., 2012). Once in the canopy, however, the average lifespan may only be 150–200 years (Hobi *et al*., 2014). European beech forests are subject to single-tree mortality and therefore expected to demonstrate small-scale gap dynamics (Tabaku and Meyer, 1999; Splechtna *et al*., 2005; Westphal *et al*., 2006). Whereas large-scale disturbances would be expected to create a mosaic on a landscape scale, single-tree mortality-driven gap dynamics should be characterized by high structural variability on the scale of one to a few trees, with structural variability declining with increasing scale and attaining relative homogeneity at larger scales. Indeed, these forests are typically described as having high structural diversity and complex uneven-aged structures reflected in a small-scale patch mosaic formed by tree mortality in 40–140 m^2 extents of one to three trees (Tabaku and Meyer, 1999; Emborg *et al*., 2000; Drößler and von Lüpke, 2005; Zeibig *et al*., 2005; Kenderes *et al*., 2008; Wagner *et al*., 2010; Rugani *et al*., 2013).

Although a number of studies have characterized several structural attributes in European temperate forests (e.g. Korpel, 1995; Smejkal *et al*., 1995; Emborg *et al*., 2000; Jaworski and Paluch, 2001; Holeska *et al*., 2009), the quantification of within-stand

structure has been limited to stand-level measures that are often inadequate for characterizing primaeval forests (Kuuluvainen *et al*., 1996; Zenner and Hibbs, 2000). In recent years, a variety of spatially explicit measures have arisen (Pommerening, 2002; von Gadow *et al*., 2012) that may shed additional light on natural developmental dynamics. Further, most intensive studies in primaeval remnant forests of European beech have been restricted to relatively small extents (e.g. 0.5–2 ha; Mayer, 1989; Leibundgut, 1993; Korpel, 1995). Few studies to date have established plots of sufficient size with known tree stem positions to enable a quantitative description of the within-stand diversity of forest structure (but see Commarmot *et al*., 2005; Král *et al*., 2010a), and none have focused on the relationships among structural measures that are sensitive to horizontal and vertical spatial diversity across scales. Nonetheless, such small extents have been the basis for characterizing the temporal dynamics of beech forests (Leibundgut, 1993; Korpel, 1995; Meyer, 1995; Tabaku, 2000; Saniga and Schütz, 2001) as composed of a mosaic of patches in different stages of the stand development cycle (Remmert, 1991; Leibundgut, 1993; Korpel, 1995). In a recent analysis of small (0.05 ha) sampling plots distributed throughout an extensive area (10 000 ha) of primaeval beech forests in the central Transcarpathian mountains, support for the kind of small-scale patch mosaic that would result from gap dynamics was seen in the spatial variability of forest canopy layering canopies across plots (Hobi *et al*., 2014).

Structural complexity, however, is known to vary with spatial scale, with some measures demonstrating area dependency (Zenner, 2005; Král *et al*., 2010a). Stem density, basal area (BA) and volume of living trees may be overestimated when extrapolating from small monitoring plots to larger extents (Holeska *et al*., 2009; Hobi *et al*., 2014), and 'old-growth' measures such as the density of large trees may have unreliable levels of variability at small scales (Zenner and Peck, 2009). Further, the fine-scale patterns reflective of development dynamics on the order of a single beech crown (ca. 156.25 m^2, Meyer, 1999), such as spatial clustering, may be overlooked in examinations of both small contiguous plots and extensive but discontinuous plots. We therefore asked the question: does the structural characterization of primaeval beech forest based on small extents and across dispersed monitoring plots still hold when examining a spatially contiguous area of relatively large extent, and if so, at what scales? Our approach was to intensively explore the scale dependency of structural complexity in the living tree stratum of a 10-ha portion of an unmanaged nearly monospecific primaeval European beech stand in the central Transcarpathian mountains. In this paper, we used the pattern of change in associations among structural measures within increasing scale to explore development dynamics.

Methods

Site description

The Uholka-Shyrokyi Luh reserve in the Carpathian Biosphere Reserve is situated on the southern slopes of the Krasna mountain range (400–1400 m a.s.l.) in central Transcarpathia, the south-westernmost region of the Ukraine. Almost 9000 ha of the 16 000 ha of European beech (*F. sylvatica* L.) dominated forests in the Carpathian Biosphere Reserve are considered to be virgin forest of almost pure European beech (Brändli *et al*., 2008). The geology of the massif is characterized by flysch formations from the Cretaceous and Palaeogene periods and is comprised of Jurassic limestone, calcareous conglomerates, marls and sandstone. The climate is temperate, with a mean temperature recorded at a nearby meteorological station at 430-m altitude of 7.7°C (−2.7°C in January, and 17.9°C in July) and an annual precipitation of 1134 mm, of which 50–60 per cent falls between May and October (Hamor and Brändli, 2013).

Experimental design

A 10-ha (200 × 500 m) inventory plot was established in the south of the Uholka-Shyrokyi Luh reserve in 2000; the data reported here reflect a remeasurement conducted in 2010. The inventory plot is located on a southeasterly exposed slope of 20–40 per cent at an altitude of 700–800 m (48°16′N, 23°37′E). The soils are mainly dystric cambisols with interspersed eutric cambisols (Commarmot *et al*., 2005), and the main forest associations are *Fagetum dentariosum* and *F. asperulosum* (Stojko *et al*., 1982). In 2000, the old-growth inventory plot was comprised of almost pure (∼97 per cent) European beech, with some *Acer pseudoplatanus* and *A. platanoides* (2.1 per cent), *Fraxinus excelsior* (0.6 per cent) and *Ulmus glabra* (0.4 per cent) present (Commarmot *et al*., 2005). On the inventory plot, all live trees with a minimum diameter at breast height ($d_{1.3}$) of 6 cm were numbered, and their positions (azimuth and distance from plot centre using a compass and tape), species and $d_{1.3}$ were recorded.

Sampling

The stem position maps were used for a computer-simulated placement of plots of different sizes. A grid of decreasing mesh size was placed over the 10-ha inventory plot to create a fixed, non-overlapping net of square subplots of the following sizes: 100 × 500 m (5 ha, $n = 2$), 100 × 250 m (2.5 ha, $n = 4$), 100 × 100 m (1 ha, $n = 10$), 50 × 100 m (5000 m^2, $n = 20$), 50 × 50 m (2500 m^2, $n = 40$), 25 × 50 m (1250 m^2, $n = 80$), 25 × 25 m (625 m^2, $n = 160$), 12.5 × 25 m (312.5 m^2, $n = 320$), and 12.5 × 12.5 m (156.25 m^2, $n = 640$). A minimum grid size of 12.5 × 12.5 m was chosen because this has been found to correspond with the projected crown area of a mature beech tree (Meyer, 1999). For each subplot, we computed the following non-spatially explicit structural measures for living trees: BA (m^2 ha^{-1}), stem density (TPHA, stems ha^{-1}), mean tree diameter (DBH, cm), the standard deviation of tree diameters (STD, cm) and the Gini coefficient (GC, Gini, 1912). Three spatially explicit indices of structural complexity were also computed for all subplots that contained at least two trees: the tree size (diameter) differentiation index (*T*, Füldner, 1995), the structural complexity index (SCI, Zenner and Hibbs, 2000) and the index of aggregation (*R*, Clark and Evans, 1954).

GC characterizes the inequity in the distribution of BA among trees (Table 1). GC is a non-spatially explicit estimator of the size dispersion of an entire size distribution that is less influenced by extreme values than the STD and, unlike the STD, is not relative to a specific measure of central tendency (e.g. the arithmetic mean). Whereas a low STD indicates that the data points tend to be very close to the average and a high STD indicates that the data points are spread out over a large range of values, a low GC indicates that all trees are similarly sized and a high GC indicates that sizes are unequally distributed among trees. GC quantifies size dispersion and has been found to discriminate well among different diameter distributions (e.g. Lexerød and Eid, 2006).

R characterizes the horizontal spatial tree distribution pattern, expressing the extent to which the observed spatial pattern of trees in a forest stand diverges from a completely spatially randomized (CSR) distribution of trees (Table 1). To test whether the calculated *R* values deviated statistically significantly from a random (Poisson) point pattern, a *z*-test was used:

$$z = \frac{r_A - r_E}{\sigma_{r_E}} = \frac{r_A - r_E}{\frac{0.26136}{\sqrt{N \cdot \frac{N}{A}}}} \quad (1)$$

Table 1 Gini coefficient and spatially explicit metrics investigated in this study

Equation	Description
Gini coefficient GC (Lexerød and Eid, 2006) $GC = \frac{\sum_{j=1}^{n}(2j - n - 1)ba_j}{\sum_{j=1}^{n} ba_j(n-1)}$ Range: 0 (complete equality) to 1. Measure of inequality of values in a distribution.	GC is an estimate of the divergence from a perfect 1:1 line of the cumulative distribution of ranked BAs against stem numbers, where ba_j is the BA of tree in rank j, n is the total number of trees in the subplot and j is the rank of a tree in order from 1 to n.
Index of Aggregation R (Clark and Evans, 1954) adjusted for edge effects and spatial dependency when all nearest neighbours are used (Donnelly's, 1978): $R = \frac{r_A}{r_E} = \frac{\frac{1}{n}\sum_{i=1}^{n} r_i}{0.5 \cdot \left(\frac{A}{n}\right)^{\frac{1}{2}} + 0.0514 \cdot \frac{P}{n} + 0.041 \cdot \frac{P}{n^{\frac{3}{2}}}}$ Range: 0 (at maximum tree clustering) to 2.1491 (at a regular hexagonal arrangement of trees), 1 indicates a random spatial distribution, values significantly >1 indicate regularity, values significantly <1 indicate clustering. Measure of horizontal structure.	R is the observed average distance of all trees to their respective nearest neighbour (r_A) divided by the expected mean distance under a random or Poisson spatial distribution (r_E): r_i is the distance between tree i and its nearest neighbour (in metres), n is the total number of trees in the sample subplot, A is the area of the plot and P its perimeter.
Diameter Differentiation Index T (Füldner, 1995): $T = \frac{1}{n}\sum_{i=1}^{n}\frac{1}{4} \cdot \sum_{j=1}^{4}\left[1 - \frac{\mathrm{MIN}(DBH_i,\ DBH_j)}{\mathrm{MAX}(DBH_i,\ DBH_j)}\right]$ Range: 0 to 1. Surrogate measure of vertical structure.	T is the plot average of the average size (DBH) difference of the $n = 4$ nearest neighbours j of each individual reference tree i, n is the total number of trees in the sample subplot. Although based on tree diameters, T is considered a measure of vertical structure because of the strong correlation between tree diameter and height (Assmann, 1970).
Structural Complexity Index SCI (Zenner and Hibbs, 2000): $SCI = \sum_{i=1}^{n}\frac{1}{2} \cdot \frac{\left\|\begin{bmatrix} x_b - x_a \\ y_b - y_a \\ z_b - z_a \end{bmatrix}_i \times \begin{bmatrix} x_c - x_a \\ y_c - y_a \\ z_c - z_a \end{bmatrix}_i\right\|}{\left\|\begin{bmatrix} x_b - x_a \\ y_b - y_a \end{bmatrix}_i \times \begin{bmatrix} x_c - x_a \\ y_c - y_a \end{bmatrix}_i\right\|}$ Range: ≥1 (1 when all trees are the same size, regardless of spatial pattern; no upper bound). Measure of horizontal and vertical structure.	SCI is the sum of the surface areas of TINs in x–y–z-space divided by the projected ground area of all triangles in x–y-space: x, y and z (DBH) are the coordinates of trees in three dimensions, subscripts a, b and c are trees within a triangle i, n is the number of non-overlapping triangles in the sample subplot and SCI is the product of the vectors AB and AC. Possible edge effects were corrected by first creating a buffer area outside the 10-ha plot (toroidal wrap) to avoid non-equilateral triangles at the plot edge and then omitting triangles connected to trees located in the buffer area.

If $|z|$ is <1.96, trees are considered randomly distributed, z-values below −1.96 indicate a clustered pattern and z-values of >1.96 indicate a uniform pattern.

T is a surrogate for vertical size differentiation that quantifies the size difference (based on diameter) between a focal tree and its four nearest neighbours (Table 1). Because each tree in a plot serves, in turn, as a focal tree, the average T measures small-scale size dispersion relative to every tree in a plot. In contrast to STD, which quantifies dispersion relative to the arithmetic mean of tree sizes, and to GC, which quantifies the dispersion of tree sizes in the entire distribution, T quantifies the dispersion of tree sizes in the small neighbourhood relative to every tree. T has been found to distinguish very well between differentially heterogeneous structures in stands characterized by even-sized and uneven-sized diameter distributions (e.g. Zenner *et al.*, 2011).

SCI characterizes the three-dimensional structure of live trees and reflects both spatial positioning and tree size differentiation (Table 1). Spatial tessellation of spatially mapped trees creates a triangulated irregular network (TIN) of Delaunay triangles of horizontally adjacent tree neighbours (x, y) and, using the diameter of each tree as the vertical (z) dimension in each triangle, creates a rumpled surface that is shaped by the horizontal distribution of differentially sized trees in space. SCI quantifies the cumulative dispersion of tree sizes in the entire plot by summing the local size differences of each tree to its 6–8 nearest Delaunay triangle neighbours over the entire plot. SCI has been found to distinguish well between differentially heterogeneous structures in stands characterized by even-sized and uneven-sized diameter distributions (e.g. Zenner *et al.*, 2011) and, because there is no upper bound, enables comparisons of the levels of the three-dimensional structural complexity of different forest types (Zenner and Hibbs, 2000). Spatial tessellation and computations of all metrics were performed in Matlab V.8.2 (Mathworks, Inc., 2013).

Statistical analyses

Because STD, *T*, GC and SCI measure different aspects of tree size dispersion in a stand and the SCI is the most comprehensive measure of three-dimensional structure that takes into account both the horizontal spatial dispersion and the vertical size dispersion of trees on a plot, we used the change in the associations across scales between the SCI and STD, *T* and GC to assess which measures of tree size dispersion were most strongly related to three-dimensional structure at different scales.

Associations among structural measures were assessed separately for each scale using Spearman rank correlation analysis due to significant departures from normality of several structural measures. Statistical significance was assessed with 1000 Monte Carlo estimates (permutation tests) of the exact *P*-value for the Spearman correlation coefficient. Because our sampling design consists of lattice data (i.e. square quadrats over the 10-ha study area), we first assessed the presence of small-scale spatial dependence (i.e. spatial autocorrelation) on the SCI (Littell *et al.*, 2006). We assessed several covariance models using the −2 Res Log Likelihood fit statistic and determined that the Gaussian covariance structure provided the best fit for our data. To test for the existence of spatial variability, we compared the −2 Res Log Likelihood fit statistics of the Gaussian covariance model to that of the independent errors model and used a χ^2 test with 2 degrees of freedom (Littell *et al.*, 2006). Because there was no evidence of significant spatial variability at any scale (all $P > 0.9$), we report ordinary least squares (OLS) multiple regression results. OLS allows a more intuitive assessment of the change in relative contribution of structural measures (BA, TPHA, DBH, STD, GC, *R* and *T*) to the structural complexity index (SCI) at each scale up to 1 ha with partial R^2.

Multicollinearity is severe at variance inflation factors (VIF) of >10 (Neter *et al.*, 1996); in this study, multicollinearity was not a problem because VIF values for variables in the regression model exceeded 2.5 only in two models (at the scales of 156.25 and 312.5 m^2, the VIF for STD was 5.1 and 3.4, respectively). Natural logarithmic transformation was applied to the SCI to linearize regression models. Predicted values were plotted against observed values to ensure that residuals did not show systematic trends. The reported final model was the subsequent candidate model with the lowest Akaike's Information Criterion adjusted for small sample size (AIC_c), based on a spatial exponential covariance matrix (Burnham and Anderson, 2002). Principal components analysis (PCA in *PC-ORD* v. 6.14, McCune and Mefford, 2011) using correlation coefficients in the cross-products matrix was further used to summarize the strongest linear patterns among structural measures separately for each scale up to 1 ha. Only significant (randomization test, alpha = 0.05) axes are reported.

Results

At the 10-ha scale, the spatially randomly ($R = 1.018$) distributed 292.6 TPHA comprised a BA of 37.5 m^2 (95.5 per cent of which was beech) with a mean DBH of 29.5 cm and an STD of 27.7 cm. The forest exhibited a rotated sigmoid diameter distribution (Figure 1) and incorporated 23.3 large trees per ha with a DBH of 80 cm or more (maximum DBH 129.9 cm), had a GC of 0.72, a *T* of 0.45 and an SCI of 7.43. At the 156.25-m^2 scale, we observed 12 (1.9 per cent) and 45 (7 per cent) grid cells with none or only one tree, respectively, and at the 312.5-m^2 scale, two (0.6 per cent) grid cells contained only one tree for which no estimates of variability (STD and GINI) or spatially explicit metrics could be computed. Across scales, the ranges of all structural measures predictably decreased with increasing scale (i.e. with decreasing sample size) as expected (Table 2).

The vast majority (83–90 per cent) of subplots exhibited random spatial distributions of trees at all scales (*R* not statistically significantly different from 1). Regularity increased with increasing scale, gradually between the 156.25-m^2 (0.3 per cent of all subplots) and 1250-m^2 scales (1.3 per cent) and then suddenly at the 2500-m^2 scale (7.5 per cent), maxing out at 10 per cent at the 1-ha scale. Spatial clustering showed the opposite pattern, with no clustering at the two largest scales, 10 per cent clustering at the 2500-m^2 scale, 12.5 per cent at the 1250-m^2 and 625-m^2 scales, and just under 15 per cent of all subplots at the two smallest scales.

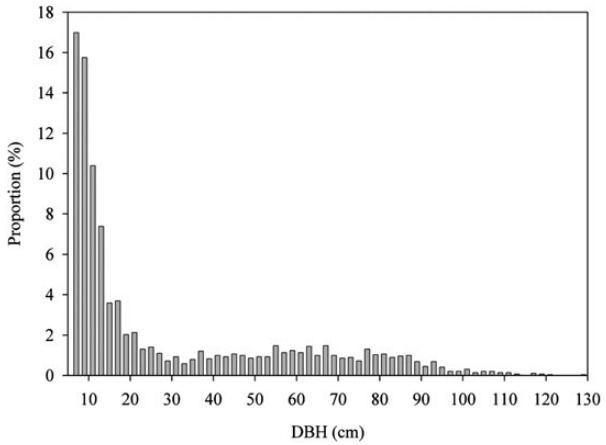

Figure 1 Frequency distribution (in %) of trees of ≥6 cm diameter at breast height over the 10-ha study site. Diameter classes are 2 cm wide.

The patterns and strengths of associations among structural measures differed among scales (Table 3). Associations between BA and DBH, STD, *T* and SCI were consistently moderately ($|r| > 0.25$) to strongly positive ($|r| > 0.5$) across all scales of <1 ha, and moderately negative with GC at scales of >625 m^2. Subplots with more BA tended to be comprised of trees with higher average tree DBHs, greater size variability (STD), larger size differences among neighbours (*T*), tree distributions with less size inequity (GC) at scales of >625 m^2 and a higher structural complexity (SCI) across scales.

Associations between TPHA and DBH and *T* were strongly and moderately negative at most scales, respectively, whereas its association with STD became strongly negative with increasing scale (>1250 m^2) and strongly positive with GC at scales between 625 and 5000 m^2. Subplots with higher tree densities tended to have a lower average DBH, smaller size differences among neighbours (*T*) and lower size variability (STD) at scales of >1250 m^2. TPHA was moderately positively associated with *R* at scales up to 625 m^2, indicating that subplots with higher tree densities tended to exhibit less intensive clustering and more random spatial structures at these scales.

DBH was moderately to strongly positively associated with STD and *T* and strongly negatively associated with GC at all but the smallest scales, indicating that subplots with a greater average DBH exhibited greater size variation (STD) and larger size differences among neighbours (*T*), but overall less size inequity among trees (GC). STD was at least moderately positively correlated with GC at scales of ≤312.5 m^2 and its strongly positive association with both *T* and SCI degraded gradually with increasing scale until it was non-significant after 2500 m^2. Subplots with a greater STD exhibited greater overall tree size inequity (GC) only at small scales and larger size differences among neighbours (*T*) and a higher structural complexity (SCI) at scales of ≤2500 m^2.

Table 2 Mean (standard error) and range (minimum – maximum observed value) of measures of forest structure at different scales

Independent variable	Scale (m^2)						
	156.25 ($N = 640$)	312.5 ($N = 320$)	625 ($N = 160$)	1250 ($N = 80$)	2500 ($N = 40$)	5000 ($N = 20$)	10 000 ($N = 10$)
BA	37.5 (1.10) (0–142)	37.5 (1.13) 0.2–111.4	37.5 (1.13) (8–83.5)	37.5 (1.07) (16.8–55)	37.5 (1.18) (21.7–51)	37.5 (1.29) (26.3–48.1)	37.5 (1.39) (30.6–43.7)
TPHA	292.6 (6.7) (0–1024)	292.6 (7.4) (32–768)	292.6 (8.8) (64–592)	292.6 (9.8) (112–536)	292.6 (11.3) (148–460)	292.6 (12.2) (210–388)	292.6 (14.7) (232–366)
DBH	34.6 (0.8)[a] (6.3–110.3)	33.1 (0.8) (8.3–85.0)	32.3 (0.9) (13.6–74.1)	31.2 (0.9) (17.0–60.7)	30.6 (1.1) (19–54)	30.0 (0.9) (22.3–36.2)	29.8 (1.0) (22.6–32.7)
STD	23.2 (0.5)[b] (0.3–71.6)	25.4 (0.5)[c] (0.3–48.6)	26.6 (0.5) (9–39.3)	27.3 (0.5) (15–36.4)	27.4 (0.5) (18.4–33.5)	27.6 (0.6) (20.9–32.2)	27.7 (0.6) (23.5–29.7)
GC	0.65 (0.01)[b] (0–0.99)	0.68 (0.01)[c] (0.01–0.97)	0.69 (0.01) (0.17–0.88)	0.70 (0.01) (0.38–0.83)	0.70 (0.01) (0.46–0.82)	0.71 (0.01) (0.62–0.80)	0.72 (0.01) (0.68–0.78)
T	0.47 (0.01)[b] (0.09–0.77)	0.46 (0.01)[c] (0.12–0.69)	0.46 (0.01) (0.27–0.67)	0.46 (0.01) (0.34–0.62)	0.46 (0.01) (0.37–0.53)	0.45 (0.01) (0.41–0.50)	0.45 (0.01) (0.43–0.49)
SCI	8.49 (0.20)[b] (1.11–43.88)	7.81 (0.16)[c] (1.17–27.07)	7.60 (0.15) (3.41–12.30)	7.52 (0.15) (3.77–10.74)	7.46 (0.16) (5.57–9.67)	7.43 (0.17) (6.13–9.20)	7.43 (0.16) (6.61–8.18)

N = sample size; BA = basal area per hectare (m^2 ha^{-1}); TPHA = stem density ha^{-1}; DBH = average tree diameter (cm); STD = standard deviation of tree diameters (cm); GC = Gini coefficient; *T* = diameter differentiation index; SCI = structural complexity index.
[a]$N = 628$.
[b]$N = 583$.
[c]$N = 318$.

Table 3 Spearman rank correlations among stand-level structural measures and spatially explicit structural indices at different scales (m^2)

	Scale	BA	TPHA	DBH	STD	*T*	GC	*R*
TPHA	156.25	0.10						
	312.5	0.13						
	625	*0.10*						
	1250	*0.10*						
	2500	*0.08*						
	5000	*0.06*						
	10 000	*0.13*						
DBH	156.25	**0.73**	**−0.47**					
	312.5	**0.66**	**−0.57**					
	625	**0.57**	**−0.70**					
	1250	**0.50**	**−0.75**					
	2500	**0.52**	**−0.74**					
	5000	0.49	**−0.78**					
	10 000	*0.44*	*−0.62*					
STD	156.25	**0.61**	*−0.06*	**0.50**				
	312.5	**0.56**	**−0.20**	**0.50**				
	625	**0.48**	**−0.37**	**0.54**				
	1250	**0.48**	**−0.49**	**0.59**				
	2500	**0.45**	**−0.54**	**0.61**				
	5000	*0.34*	**−0.77**	**0.77**				
	10 000	*0.28*	−0.71	*0.58*				
T	156.25	**0.28**	**−0.22**	**0.33**	**0.60**			
	312.5	**0.27**	**−0.23**	**0.36**	**0.58**			
	625	**0.28**	**−0.26**	**0.38**	**0.53**			
	1250	0.25	−0.25	**0.41**	**0.37**			
	2500	0.35	−0.35	**0.60**	**0.47**			
	5000	*0.45*	*−0.38*	**0.58**	*0.39*			
	10 000	0.67	*−0.08*	*0.31*	*0.44*			
GC	156.25	*0.06*	**0.14**	**−0.14**	**0.66**	**0.39**		
	312.5	**−0.19**	**0.38**	**−0.51**	**0.30**	*0.07*		
	625	**−0.24**	**0.51**	**−0.71**	*0.05*	*−0.11*		
	1250	**−0.36**	**0.52**	**−0.82**	*−0.10*	**−0.33**		
	2500	−0.38	**0.59**	**−0.86**	*−0.21*	**−0.49**		
	5000	*−0.43*	**0.57**	**−0.85**	*−0.43*	−0.55		
	10 000	*−0.46*	*0.42*	**−0.79**	*−0.14*	*−0.35*		
R	156.25	**0.19**	**0.33**	*−0.02*	*0.08*	*0.04*	*0.05*	
	312.5	**0.22**	**0.38**	*−0.08*	*0.03*	*0.03*	*0.09*	
	625	0.20	**0.28**	*−0.07*	*0.00*	*0.13*	*0.10*	
	1250	*0.14*	*0.12*	*−0.01*	*−0.02*	0.27	*−0.04*	
	2500	*−0.04*	*−0.01*	*0.07*	*−0.02*	0.32	*−0.15*	
	5000	*0.09*	*−0.01*	*−0.04*	*0.06*	*0.32*	*−0.14*	
	10 000	*0.35*	*0.02*	*−0.25*	*0.07*	*0.54*	*−0.10*	
SCI	156.25	**0.60**	*0.05*	**0.41**	**0.80**	**0.61**	**0.51**	*0.00*
	312.5	**0.56**	0.13	**0.28**	**0.70**	**0.57**	**0.30**	*0.04*
	625	**0.54**	0.18	*0.14*	**0.60**	**0.53**	**0.24**	*0.12*
	1250	**0.54**	0.24	*0.05*	**0.48**	**0.40**	*0.19*	*0.06*
	2500	**0.67**	0.38	*0.07*	0.32	**0.40**	*0.10*	*0.06*
	5000	**0.72**	*0.39*	*−0.01*	*0.05*	0.45	*0.08*	*0.15*
	10 000	0.66	*0.62*	*−0.25*	*−0.05*	*0.53*	*0.18*	*0.51*

Statistical significance is indicated by italic ($P > 0.05$), regular ($0.05 \leq P < 0.01$) or bold ($P \leq 0.01$) text. At larger scales of 0.5 and 1 ha, even strongly positive or negative correlations may not be statistically significant due to low samples sizes ($N = 20$ and 10, respectively).
BA = basal area per hectare (m^2 ha^{-1}); TPHA = stem density per hectare; DBH = mean stand diameter at breast height (cm); STD = standard deviation of tree diameters (cm); *T* = diameter differentiation index; GC = Gini coefficient; *R* = index of aggregation; SCI = Structural Complexity Index.

Somewhat similarly, the association between GC and *T* was moderately positive only at the smallest scale, weak at intermediate scales and at least moderately negative at scales of ≥1250 m^2, indicating that subplots with greater overall tree size inequity (GC) exhibited larger size differences among neighbours (*T*) only at the smallest scales and smaller size differences among neighbours at larger scales. Associations between SCI and GC and *T* were strongly positive only at the smallest (GC) or up to 625 m^2 (*T*) and decreased with increasing scale, indicating that subplots with higher structural complexity had larger size differences among neighbours (*T*) and greater overall tree size inequity (GC), particularly at smaller scales.

The most consistent predictor of structural complexity (SCI) across scales (Table 4) was the positive contribution of BA, which increased in importance with increasing scale. Similarly, GC was also an increasingly important positive predictor of structure with increasing scale. The positive contribution of *T* peaked at scales between 1250 and 5000 m^2, whereas the weak negative contribution of *R* was only significant at scales of ≤312.5 m^2 and the strong positive contribution of STD was only seen at the smallest scales (≤625 m^2).

These patterns of association among structural measures across scales are summarized in the PCA ordination diagram (Figure 2). At all scales, the strongest linear trend (all $P \leq 0.02$, 37–50 per cent increasing with increasing scale) contrasted subplots with high DBH and those with high TPHA. The second strongest linear trend (all $P < 0.05$, 23–29 per cent) varied somewhat across scale, initially reflecting variations in GC but increasingly capturing the gradient in SCI as scale increased (>312.5 m^2). At all scales, the third strongest linear trend ($P < 0.01$ only ≤625 m^2, 17–8 per cent decreasing with increasing scale) was a gradient in *R*. Several patterns evolved with increasing scale. First, the association of BA with the structure gradient remained stable across all scales even as other associations declined, increasing the relative contribution of BA with scale. Second, the contribution of STD was very strong at the smallest scales but decreased particularly by 1250 m^2. Third, the trajectories of STD and *T* were initially similar and then diverged after the 2500-m^2 scale as the contribution of STD continued to decline. Finally, the relative contribution of GC shifted with increasing scale until its contribution was the inverse of STD.

Discussion

This study explored variation in structural measures across spatial scales ranging from the stand level (10 ha) down to the approximate extent of the projected crown area of a single mature beech tree (156.25 m^2, Meyer, 1999). The observed patterns of large ranges of all measures of forest structure at small scales, similar levels of variability of all measures of heterogeneity of tree sizes with increasing scale and dependence of structural complexity on measures of fine-scale variability at small scales were consistent with the fine-scale shifting mosaic of patches in different development stages previously associated with primaeval European beech forests (Leibundgut, 1982; Remmert, 1991; Korpel, 1995; Emborg *et al.*, 2000; Král *et al.*, 2010b).

The forest structures observed in 2010 within the 10-ha sampling plot in the Uholka-Shyrokyi Luh reserve were typical of primaeval beech forest in east-central Europe (e.g. Slovakia, Ukraine), for which similar BAs (32–47 m^2 ha^{-1}), tree densities (225–350 trees ha^{-1}) and mean tree sizes (27–29 cm) have been reported (Korpel, 1995; Drößler, 2006). As has been previously indicated by age and disturbance reconstructions (Trotsiuk *et al.*, 2012) and is characteristic of European beech forests (Tabaku and Meyer, 1999; Rugani *et al.*, 2013), the results reported here provide little evidence of large historic disturbances. The rotated sigmoid diameter distribution is typical not only of virgin beech forest (Korpel, 1995; Tabaku, 2000; Westphal *et al.*, 2006) but of old-growth in general (Goff and West, 1975). The forests in Uholka are in fact known to contain trees of >400 years in age (Trotsiuk *et al.*, 2012), with trees of comparable diameter easily spanning 100 – and even 200 – years in age (Trotsiuk *et al.*, 2012). These widely temporally spaced trees occur in close proximity to one another; an age span of 470 years has been observed in a single nearby 0.1-ha plot (Trotsiuk *et al.*, 2012). This extreme heterogeneity at small spatial scales, with high levels of canopy layering, was reflected in the current study in the large ranges of all structural measures at the smallest (one- to two-crown) scales. Nonetheless, despite this high variability, some consistent structural patterns emerged across all scales: (1) BA and tree density were never significantly correlated, indicating a lack of clear separation of regeneration patches, with many small trees and low BAs, from areas

Table 4 Partial coefficients of determination (R^2) for the regression models with the lowest Akaike's information criterion adjusted for small sample size (AIC_c) for the structural complexity index (SCI, ln-transformed) against the other structural measures for each scale

Independent variable	Scale (m^2)						
	156.25	312.5	625	1250	2500	5000	10 000
R	− *** 0.018	− ** 0.007	n.s.	n.s.	n.s.	n.s.	n.s.
STD	+ *** 0.600	+ *** 0.557	+ *** 0.456	+ * 0.017	n.s.	n.s.	n.s.
T	+ *** 0.034	+ *** 0.032	+ *** 0.057	+ *** 0.113	+ *** 0.102	+ ** 0.089	n.s.
GC	+ *** 0.015	+ *** 0.075	+ *** 0.109	+ *** 0.218	+ *** 0.181	+ *** 0.254	+ * 0.274
BA	+ *** 0.023	+ *** 0.036	+ *** 0.057	+ *** 0.358	+ *** 0.527	+ *** 0.539	+ ** 0.448

R = index of aggregation; STD = standard deviation of tree diameters (cm); *T* = diameter differentiation index; GC = Gini coefficient; BA = basal area per hectare (m^2 ha^{-1}).
***$P \leq 0.001$; **$P \leq 0.01$; *$P \leq 0.05$; n.s. = not significant.
+/− indicate positive/negative estimates of the slope coefficient.

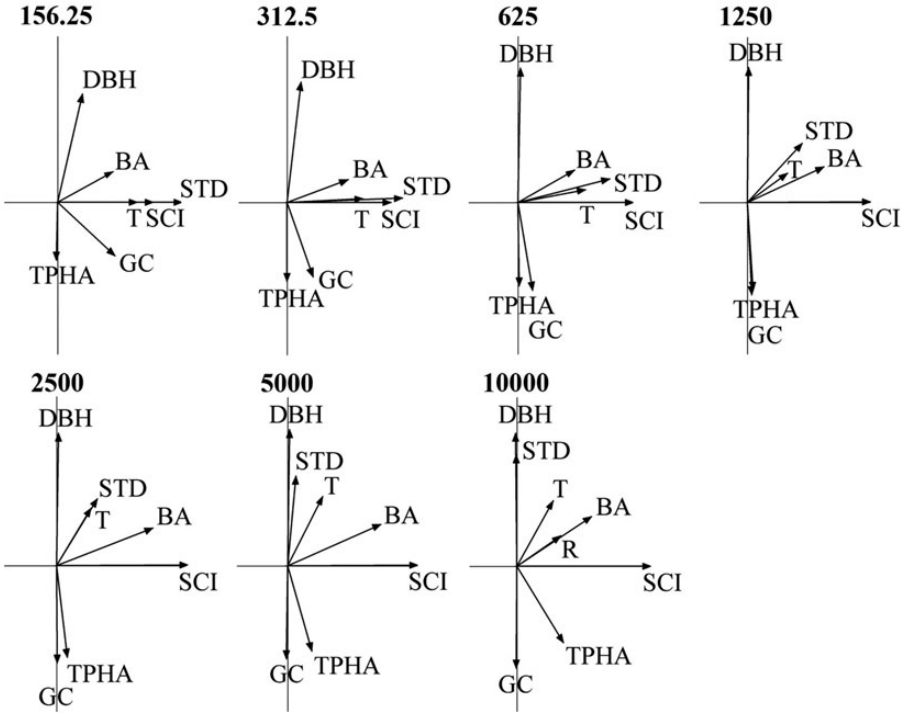

Figure 2 Principal components analysis ordination vectors for each structural measure on the first two ordination axes, by scale from 156.25 to 10 000 m^2. The percentage of variance explained increased with increasing scale (from 37 to 50 % on Axis 1, 23 to 29 % on Axis 2). BA, basal area; DBH, mean stand diameter at breast height; GC, Gini coefficient; *R*, index of aggregation; SCI, Structural Complexity Index; STD, standard deviation of tree diameters; *T*, diameter differentiation index; TPHA, stem density per hectare. For this figure, all ordinations were similarly rescaled and rotated to align the SCI gradient with the horizontal axis to facilitate comparison. In all cases, the third axis (not shown) was driven almost solely by spatial aggregation (*R*). As scale increased, STD rotated up and to the left, becoming less aligned with SCI and increasingly aligned with DBH. The diameter differentiation index (*T*) initially followed the same trajectory as STD until around the 2500-m^2 scale. On the opposite end of the vertical axis, the GC rotated down and to the left until its contribution was the inverse of STD. The relationships between DBH, BA and TPHA and the other measures remained relatively stable across scales.

with fewer yet larger trees devoid of smaller trees; (2) denser patches had lower average tree sizes (DBH), smaller size differences among neighbours and less size variability (STD) across all scales, indicating that the effect of gaps was not limited to the typically small footprint of the actual gap opening of <200 m^2 in this area (Hobi *et al.*, 2013, 2014) and (3) areas with more BA typically were comprised of larger trees (DBH) with greater size variability (STD) and larger size differences among neighbours (*T*) – yet less size inequity (GC) among all trees – than areas with lower BA at scales exceeding two crowns, indicating a relative scarcity of smaller trees in areas with more BA.

Sensitivity across scales

The small-scale developmental processes shaping the structure of this forest were reflected in the change in associations among these measures with increasing subplot size, such as the progressive deterioration of the positive association between STD and *T* with increasing scale. Because STD, GC, *T* and SCI all measure the heterogeneity of tree sizes and reflect different levels of size disparities among nearest neighbours, they all successfully revealed high between-patch differences at small scales, a sign of small-scale gap dynamics. However, as subplots increasingly incorporated more variability with increasing scale, and structural differences shifted away from size differences among nearest neighbours to more subtle overall within-patch differences, these measures began to capture different aspects of size heterogeneity and their correlations weakened. This is particularly well shown in the association between *T*, which captures spatially explicit local tree-to-tree size variation, and GC, which reflects the non-spatial collective inequity in the BA contributed by those trees. At the smallest, single-crown scale, this association was moderately positive, reflecting high small-scale heterogeneity. At larger scales, upwards of a quarter hectare, this relationship was moderately negative, reflecting the increasing disconnect between a measure sensitive to local size variation (*T*) and one capable of capturing structural variability even after the smoothing effect of converging heterogeneous tree neighbourhoods (GC). At the smallest scales, subplot-to-subplot variation consisted largely of differences in absolute size among individual trees and small groups of trees, which were captured by all three measures. At intermediate scales, subplot-to-subplot variation consisted of differences in local neighbourhood heterogeneity, which was best captured by *T* as a measure of size variability among neighbouring trees. At the larger scales in which this patch heterogeneity was collectively incorporated within the subplot, the more subtle subplot-to-subplot variation was best captured by the GC as an overall measure of inequity.

Drivers of structural complexity

The relative contribution of these measures to small-scale structural complexity as captured by the SCI also varied with scale. Under small-scale gap dynamics, at the smallest (one- to two-crown) scales where gap regeneration would lead to small clusters of relatively evenly sized trees (Rouvinen and Kuuluvainen, 2005; Paluch, 2007) in which even minor variations in tree size would be relatively important, small-scale structural complexity would be driven by the kind of tree-to-tree level variation best captured by measures of dispersion. In this case, the combination of spatial point pattern (capturing clustering) with the variability in tree diameters was most sensitive to the potential for small-scale structural complexity at the smallest scales. At intermediate scales comparable with 4–8 tree crowns, small-scale gap dynamics would be expected to create small neighbourhoods of trees that differed in their degree of size variation, and in the current study, structural complexity was best captured by the spatially explicit *T* at intermediate scales. At the larger scales equivalent to 8–64 tree crowns, a mosaic of patches in different development stages would be expected to exhibit the kind of variation that would be best captured by global summaries. Indeed, at the largest scales, small-scale structural complexity was a function of the collective differences in the macro structures of BA – the raw material of live tree structure – and GC – a measure of the distribution of that structure. As the scale of observation increased, individual tree processes coalesced into neighbourhoods and then into patches, such that the structural complexity index was best described by variations in tree size at the smallest scales and by the distribution of tree sizes at the largest scales. When the developmental processes shaping small-scale structural complexity are small in scale, whether or not we must see the forest for the trees or the trees for the forest depends upon the scale of observation.

Spatial analyses, however, must frequently make assumptions about the spatial distribution of potentially influential resources (Littell *et al*., 2006). In the current study, for instance, spatially explicit data on the distribution of the soil resource were not available. Based on the fact that the study plot was characterized by deep, relatively undifferentiated cambisols lacking layers that might introduce spatial structure, such as through differential drainage (e.g. clay), we may assume that the influence of soil variability is relatively minor. Support for this assumption is also taken from the observation that beech seedlings, although rare, were ubiquitous throughout the study plot (Commarmot *et al*., 2005). Given the capacity of beech seedlings to survive several years at very low light levels (Emborg, 1998; Wagner *et al*., 2010) and their ability to respond rapidly to increased light conditions (Newbold and Goldsmith, 1990; Peltier *et al*., 1997; Collet *et al*., 2001), we presume that the beech seedling bank, which plays an important role in developmental dynamics despite a lack of generalizable trends in spatial pattern (Szwagrzyk *et al*., 2001), was poised to rapidly fill canopy gaps within the brief 3–4 years that small-scale gaps are thought to create canopy openings (Madsen and Hahn, 2008) before they are closed by lateral crown extension (Schütz, 1998; Splechtna *et al*., 2005). It is therefore not unreasonable to presume that the observed spatial structures of trees reflect the response of the seedling bank to gap dynamics rather than merely microsite variability.

Scale of gap dynamics

The observed heterogeneity in structural complexity thus extends beyond the spatial extent of the single beech tree, or even a small group of one to three trees, thought to be typical of small-gap processes in beech forests (Drößler and von Lüpke, 2005; Kucbel *et al*., 2010). Most gaps in this area have been found to be <200 m^2 (Hobi *et al*., 2013, 2014), and typical beech gaps range from 93 to 141 m^2 in extent (Zeibig *et al*., 2005; Kenderes *et al*., 2008; Rugani *et al*., 2013). The structural imprint of the mosaic of forest patches formed by those gaps, however, is much larger. The variability in structural measures remained high even for the most sensitive measures well beyond the four-crown scale of 625 m^2 to at least the eight-crown scale of 1250 m^2. The spatial point pattern shifted from some clustering to some regularity between the eight- and sixteen-crown scales. The threshold for statistical significance in the associations among structural measures typically occurred somewhere between the four- and sixteen-crown scales. Further, the transition in the regression model from tree-to-tree sensitive measures to neighbourhood sensitive measures, and from neighbourhood sensitive measures to patch sensitive measures, took place at the four- and eight-crown scales, respectively. Further, although a mosaic of patches in different development phases could form around gaps initiated by single-tree mortality, gaps can also be expanded through windthrow (Peterken, 1996; Schelhaas *et al*., 2003; Westphal *et al*., 2006; Firm *et al*., 2009) or stem breakage following snow events (Zeibig *et al*., 2005; Firm *et al*., 2009) or due to stem rot (Pontailler *et al*., 1997), either enlarging the actual gap or allowing sufficient changes to moisture and light regimes to promote an uneven-aged structure on a larger extent than directly under the gap itself, enlarging the initial functional gap size.

We therefore conclude that the characterization of primaeval beech forests as a fine-scale shifting mosaic of patches in different development stages appears to hold not only at small extents and in dispersed monitoring plots but also when examining a spatially contiguous area of relatively large extent. Although structural complexity may not vary with scale, the coalescence of small-scale processes into neighbourhoods and patches at larger scales may be best captured by different structural measures because the structural imprint of gap dynamics extends considerably beyond the scale of individual gaps. As a consequence, managing forests towards primaeval forest structures may indeed be more successful when reproducing the variability in structure across scales rather than aiming for specific metric targets (Zenner, 2005; Král *et al*., 2010a).

Acknowledgements

We thank Yuriy Shparyk and his team from the Ukrainian Research Institute of Mountain Forestry and collaborators from the Carpathian Biosphere Reserve for field measurements. The manuscript was also improved by the suggestions of three anonymous reviewers.

Conflict of interest statement

None declared.

References

Assmann, E. 1970 *The Principles of Forest Yield Studies. Studies in the Organic Production, Structure, Increment, and Yield of Forest Stands*. Pergamon Press, 506 pp.

Bengtsson, J., Nilsson, S.G., Franc, A. and Menozzi, P. 2000 Biodiversity, disturbances, ecosystem function and management of European forests. *For. Ecol. Manag.* **132**, 39–50.

Brändli, U.-B., Dovhanych, J. and Commarmot, B. 2008 *Virgin Forest of Uholke. Nature Guide to the Largest Virgin Beech Forest of Europe. A UNESCO World Heritage Site*. Swiss Federal Research Institute WSL, Carpathian Biosphere Reserve, 24 pp.

Burnham, K.P. and Anderson, D.R. 2002 *Model Selection and Multimodal Inference: a Practical Information-Theoretic Approach*. 2nd edn, Springer, 488 pp.

Busing, R.T. and White, P.S. 1997 Species diversity and small-scale disturbance in an old-growth temperate forest: a consideration of gap partitioning concepts. *Oikos* **78**, 562–568.

Clark, P.J. and Evans, F.C. 1954 Distance to nearest neighbor as a measure of spatial relationships in populations. *Ecology* **35**, 445–453.

Collet, C., Lanter, O. and Pardos, M. 2001 Effects of canopy opening on height and diameter growth in naturally regenerated beech seedlings. *Ann. For. Sci.* **58**, 127–134.

Commarmot, B., Bachofen, H., Bundziak, Y., Bürgi, A., Ramp, B., Shparyk, Y. *et al*. 2005 Structure of virgin and managed beech forests in Uholka (Ukraine) and Sihlwald (Switzerland): a comparative study. *For. Snow Lands. Res.* **79**, 45–56.

Commarmot, B., Brändli, U-B., Hamor, F. and Lavnyy, V. (eds). 2013 Inventory of the largest virgin beech forest of Europe. A Swiss-Ukrainian scientific adventure. In *Swiss Federal Institute of Forest, Snow, and Landscape Research, Birmensdorf*. National Forestry University, L'viv, Carpathian Biosphere Reserve, Rakhiv, 69.

Donnelly, K. 1978 Simulations to determine the variance and edge effect of total nearest neighbour distance. In *Simulation Methods in Archaeology*. Hodder, J.R. (ed.). Cambridge University Press, pp. 91–95.

Drößler, L. 2006 Struktur und Dynamik von zwei Buchenurwäldern in der Slowakei. Dissertation, Georg August University of Göttingen, 101 pp.

Drößler, L. and von Lüpke, B. 2005 Canopy gaps in two virgin beech forest reserves in Slovakia. *J. For. Sci.* **51**, 446–457.

Emborg, J. 1998 Understorey light conditions and regeneration with respect to the structural dynamics of a near-natural temperate deciduous forest in Denmark. *For. Ecol. Manag.* **106**, 83–95.

Emborg, J., Christensen, M. and Heilmann-Clausen, J. 2000 The structural dynamics of Suserup Skov, a near-natural temperate deciduous forest in Denmark. *For. Ecol. Manag.* **126**, 173–189.

Firm, D., Nagel, T.A. and Diaci, J. 2009 Disturbance history and dynamics of an old-growth mixed species mountain forest in the Slovenian Alps. *For. Ecol. Manag.* **257**, 1893–1901.

Füldner, K. 1995 Zur Strukturbeschreibung in Mischbeständen. *Forstarchiv* **66**, 235–240.

Gini, C. 1912 Variabilità e mutuabilità. Reprinted. In *Memorie di Metodologica Statistica. 1955*. Pizetti, E. and Salvemini, T. (ed.). Libreria Eredi Virgilio Veschi, pp. 211–382.

Goff, F.G. and West, D. 1975 Canopy-understory interaction effects on forest population structure. *For. Sci.* **21**, 98–108.

Hamor, F. and Brändli, U-B. 2013 The Uholka-Shrokyi Luh protected massif – an overview. In *Inventory of the Largest Primeval Beech Forest in Europe – A Swiss–Ukrainian Scientific Adventure*. Commarmot, B., Brändli, U-B., Hamor, F. and Lavnyy, V. (eds). Birmensdorf, Swiss Federal Research Institute WSL; L'viv, Ukrainian National Forestry University; Rakhiv, Carpathian Biosphere Reserve, pp. 13–17.

Hobi, M.L., Ginzler, D., Commarmot, B. and Bugmann, H. 2013 Gap pattern of the largest primeval beech forest of Europe revealed by remote-sensing. In *Structure and Disturbance Patterns of the Largest European Primeval Beech Forest Revealed by Terrestrial and Remote Sensing Data*. Hobi, M.L.. Dissertation ETH Zurich, ETH No. 21195, pp. 121–147.

Hobi, M.L., Commarmot, B. and Bugmann, H. 2014 Pattern and process in the largest primeval beech forest of Europe (Ukranian Carpathians). *J. Veg. Sci.* doi: 10.1111/jvs.12234.

Holeska, J., Saniga, M., Szwagrzyk, J., Czerniak, M., Staszyńska, K. and Kapusta, P. 2009 A giant tree stand in the West Carpathians – an exception or a relic of formerly widespread mountain European forests? *For. Ecol. Manag.* **257**, 1577–1585.

Jaworski, A. and Paluch, J. 2001 Structure and dynamics of the lower mountain zone forests of primeval character in the Babia Góra Mt. *Natl Park. J. For. Sci.* **47**, 60–74.

Keane, R.E., Hessburg, P.F., Landres, P.B. and Swanson, F.J. 2009 The use of historical range and variability (HRV) in landscape management. *For. Ecol. Manag.* **258**, 1025–1037.

Kenderes, K., Mihok, B. and Standovár, T. 2008 Thirty years of gap dynamics in a Central European beech forest reserve. *Forestry* **81**, 111–123.

Korpel, S. 1995 *Die Urwälder der Westkarpaten*. Gustav Fischer, 310 pp.

Král, K., Janík, D., Vrška, T., Adam, D., Hort, L., Unar, P. *et al*. 2010a Local variability of stand structural features in beech dominated natural forests of Central Europe: implications for sampling. *For. Ecol. Manag.* **260**, 2196–2203.

Král, K., Vrška, T., Hort, L., Adam, D. and Šamonil, P. 2010b Development phases in a temperate natural spruce-fir-beech forest: determination by a supervised classification method. *Eur. J. For. Res.* **129**, 339–351.

Kucbel, S., Jaloviar, P., Saniga, M., Vencurik, J. and Klimaš, V. 2010 Canopy gaps in an old-growth fir-beech forest remnant of Western Carpathians. *Eur. J. For. Res.* **129**, 249–259.

Kuuluvainen, T., Penttinen, A., Leinonen, K. and Nygren, M. 1996 Statistical opportunities for comparing stand structural heterogeneity in managed and primeval forests: An example from boreal spruce forest in southern Finland. *Sil. Fenn.* **30**, 315–328.

Leibundgut, H. 1982 *Europäische Urwälder der Bergstufe*. Paul Haupt, 308 pp.

Leibundgut, H. 1993 *Europäische Urwälder. Wegweiser zur naturnahen Waldwirtschaft*. Paul Haupt, 260 pp.

Lexerød, N.L. and Eid, T. 2006 An evaluation of different diameter differentiation indices based on criteria related to forest management planning. *For. Ecol. Manag.* **222**, 17–28.

Littell, R.C., Milliken, G.A., Stroup, W.W., Wolfinger, R.D. and Schabenberger, O. 2006. *SAS® for Mixed Models*. 2nd edn. SAS Institute.

Madsen, P. and Hahn, K. 2008 Natural regeneration in a beech-dominated forest managed by close-to-nature principles – a gap cutting based experiment. *Can. J. For. Res.* **38**, 1716–1729.

Mayer, H. 1989 *Urwaldreste, Naturwaldreservate und schützenswerte Naturwälder in Österreich*. 2nd edn. Institut für Waldbau, Universität für Bodenkultur, 971 pp.

McCune, B. and Mefford, M.J. 2011 *PC-ORD. Multivariate Analysis of Ecological Data*. Version 6.14. MjM Software.

Meyer, P. 1995 *Untersuchung waldkundlicher Entwicklungstendenzen und methodischer Fragestellungen in Buchen- und Buchenmischbeständen niedersächsischer Naturwaldreservate (NWR)*. Cuvillier, 303 pp.

Meyer, P. 1999 Bestimmung der Waldentwicklungsphasen und der Texturdiversität in Naturwäldern. *Allg. Forst-u. J.-Ztg* **170**, 203–211.

Mori, A.S. 2011 Ecosystem management based on natural disturbances: hierarchical context and non-equilibrium paradigm. *J. Appl. Ecol.* **48**, 280–292.

Nagel, T.A., Svoboda, M. and Diaci, J. 2006 Regeneration patterns after intermediate wind disturbance in an old-growth *Fagus-Abies* forest in southeastern Slovenia. *For. Ecol. Manag.* **226**, 268–278.

Nagel, T.A., Zenner, E.K. and Brang, P. 2013 Research in old-growth forests and forest reserves: implications for integrated forest management. In *Integrative Approaches as an Opportunity for the Conservation of Forest Biodiversity*. Kraus, D. and Krumm, F. (eds). European Forest Institute, pp. 44–50.

Neter, J., Kutner, M.H., Nachtsheim, C.J. and Wasserman, W. 1996 *Applied Linear Statistical Models: Regression, Analysis of Variance, Experimental Designs*. Irwin, 1408 pp.

Newbold, A.J. and Goldsmith, E.B. 1990 *The regeneration of oak and beech: a literature review. Discussion papers in conservation No. 33*. University College London, London.

Paluch, J.G. 2007 The spatial pattern of a natural European beech (*Fagus sylvatica* L.) – silver fir (*Abies alba* Mill.) forest: a patch mosaic perspective. *For. Ecol. Manag.* **253**, 161–170.

Peltier, A., Touzet, M.C., Armengaud, C. and Ponge, J.F. 1997 Establishment of *Fagus sylvatica* and *Fraxinus excelsior* in an old-growth beech forest. *J. Veg. Sci.* **8**, 13–20.

Peterken, G.F. 1996 *Natural Woodland Ecology and Conservation in Northern Temperate Regions*. Cambridge University Press, 525 pp.

Peters, R. 1997 Beech Forests. *Geobotany*. Vol. **24**. Springer, 170 pp.

Pommerening, A. 2002 Approaches to quantifying forest structures. *Forestry* **75**, 305–324.

Pontailler, J-Y., Faille, A. and Lemée, G. 1997 Storms drive successional dynamics in natural forests: a case study in Fontainebleau forest (France). *For. Ecol. Manag.* **98**, 1–15.

Remmert, H. 1991 The mosaic-cycle concept of ecosystems – an overview. In *The Mosaic-Cycle Concept of Ecosystems*. Remmert, H. (ed.). Springer, pp. 1–21.

Rouvinen, S. and Kuuluvainen, T. 2005 Spatial patterns of trees of different size in boreal *Pinus sylvestris* forest sites with different fire histories. *Community Ecol.* **6**, 1–12.

Rugani, T., Diaci, J. and Hdladnik, D. 2013 Gap dynamics and structure in two old-growth beech forest remnants in Slovenia. *Plos One*. **8**, e52641.

Saniga, M. and Schütz, J.P. 2001 Dynamics of change in dead wood share in selected beech virgin forests in Slovakia within their development cycle. *J. For. Sci.* **47**, 557–565.

Schelhaas, M-J., Nabuurs, G-J. and Schuck, A. 2003 Natural disturbances in the European forests in the 19th and 20th centuries. *Global Change Biol.* **9**, 1620–1633.

Schütz, J-P. 1998 Licht bis auf den Waldboden: Waldbauliche Möglichkeiten zur Optimierung des Lichteinfalls imWalde. *Schweiz. Z. Forstwes.* **150**, 478–483.

Smejkal, G.M., Bindiu, C. and Visoiu-Smejkal, D. 1995 *Banater Urwälder ökologische Untersuchungen in Rumänien*. Mirto, 198 pp.

Spies, T.A. 2004 Ecological concepts and diversity of old-growth forests. *J. For.* **102**, 14–20.

Splechtna, B.E., Gratzer, G. and Black, B.A. 2005 Disturbance history of a European old-growth mixed-species forest – a spatial dendro-ecological analysis. *J. Veg. Sci.* **16**, 511–522.

Stojko, S.M., Tasjenkevych, L.O., Milkina, L.I., Malynovskyj, K.A., Tretjak, P.R., Manko, M.P. *et al.* 1982 *Flora I roslynnist' Karpats'koho Zapovidnyka*. Naukova Dumka, 222 pp.

Szwagrzyk, J., Szewczyk, J. and Bodziarczyk, J. 2001 Dynamics of seedling banks in beech forest: results of a 10-year study on germination, growth and survival. *For. Ecol. Manag.* **141**, 237–250.

Tabaku, V. 2000 Struktur von Buchen-Urwäldern in Albanien im Vergleich mit deutschen Buchen-Naturwaldreservaten und –Wirtschaftswäldern. Dissertation, Cuvillier, 206 pp.

Tabaku, V. and Meyer, P. 1999 Lückenmuster albanischer und mitteleuropäischer Buchenwälder unterschiedlicher Nutzungsintensität. *Forstarchiv* **70**, 87–97.

Trotsiuk, V., Hobi, M.L. and Commarmot, B. 2012 Age structure and disturbance dynamics of the relic virgin beech forest Uholka (Ukrainian Carpathians). *For. Ecol. Manag.* **265**, 181–190.

Turner, M.G. 1989 Landscape ecology: the effect of pattern on process. *Annu. Rev. Ecol. Syst.* **20**, 171–197.

von Gadow, K., Zhang, C., Wehenkel, C., Pommerening, A., Corral-Rivas, J., Korol, M. *et al.* 2012 Forest structure and diversity. In *Continuous Cover Forestry*. Pukkala, T. and von Gadow, K. (ed.). Springer, pp. 29–83.

Wagner, S., Collet, C., Madsen, P., Nakashizuka, T., Nyland, R.D. and Sagheb-Talebi, K. 2010 Beech regeneration research: From ecological to silvicultural aspects. *For. Ecol. Manag.* **259**, 2172–2182.

Westphal, C., Tremer, N.v., Oheib, G., Hansen, J.v., Gadow, K. and Härdtle, W. 2006 Is the reverse J-shaped diameter distribution universally applicable in European virgin beech forests? *For. Ecol. Manag.* **223**, 75–83.

Zeibig, A., Diaci, J. and Wagner, S. 2005 Gap disturbance patterns of a *Fagus sylvatica* virgin forest remnant in the mountain vegetation belt of Slovenia. *For. Snow Lands. Res.* **79**, 69–80.

Zenner, E.K. 2005 Investigating scale-dependent stand heterogeneity with structure-area-curves. *For. Ecol. Manag.* **209**, 87–100.

Zenner, E.K. and Hibbs, D. 2000 A new method for modeling the heterogeneity of forest structure. *For. Ecol. Manag.* **129**, 75–87.

Zenner, E.K. and Peck, J.E. 2009 Characterizing structural conditions in mature managed red pine: spatial dependency of metrics and adequacy of plot size. *For. Ecol. Manag.* **257**, 311–320.

Zenner, E.K., Lähde, E. and Laiho, O. 2011 Contrasting the temporal dynamics of stand structure in even- and uneven-sized *Picea abies* dominated stands. *Can. J. For. Res.* **41**, 289–299.